A R C H I V E O F M E C H A N I C A L E N G I N E E R I N G

VOL. LXV 2018 Number 3

DOI: 10.24425/124489

Key words: turbulence models, vortex breakdown, delta wing, vortex core, CFD, roll-up vortex

SETYAWAN BEKTI WIBOWO[1,2], *SUTRISNO*[1], *TRI AGUNG ROHMAT*[1]

AN EVALUATION OF TURBULENCE MODEL FOR VORTEX BREAKDOWN DETECTION OVER DELTA WING

An important phenomenon of delta wing is the mechanism of vortex core, which indicates the increase in lifting force until the occurrence of the vortex breakdown. The computational fluid dynamics (CFD) is very helpful in visualizing and providing analysis of the detailed data. The use of turbulent models will affect the quality of results in obtaining the vortex breakdown phenomenon. This study used several models of turbulence to capture the occurrence of vortex breakdown and compare it with experiments using water tunnel test facility. The results show that all turbulence models give good results at a low angle of attack (AoA), but at a high AoA the DES model gives the results closest to experimental ones with Cl error value of about 1%. Taking into account the time required and the acceptable level of accuracy, the use of SST and k-ω models is an alternative option for use in the detection of vortex breakdown.

1. Introduction

Fighter technology is always evolving to improve efficiency and flying capabilities. In high-speed aircraft, such as fighter aircraft, the wing configuration uses a delta type. In addition to avoiding damage caused by shock waves at supersonic speeds, the use of delta wings allows one to increase the lift force especially at a high angle of attack (AoA). The delta wings can improve good maneuverability and agility. At high angles of attack, the delta wings produce greater lift and better stability compared to rectangular wings [1]. In the delta wing, the wind will stream towards the leading edge and then partially flow down and up through the wing

[1]*Department of Mechanical and Industrial Engineering, Faculty of Engineering, Universitas Gadjah Mada 55281, Indonesia. E-mail: setyawanbw@ugm.ac.id*

[2]*Department of Mechanical Engineering, Vocational College, Universitas Gadjah Mada, Yogyakarta 55281, Indonesia.*

surface. Due to the pressure difference between the top and bottom side of the wing, a roll-up vortex will form from the underside of the wing to the top of the wing surface, which will result in an increased lifting force [2]. The total lift force that occurs is the sum of the potential lift and a vortex lift increment. In the area above the wing, the lowest pressure will appear and cause the occurrence of vortex cores as the location of the highest lift. Surfaces on the wings greatly affect the formation of vortices that will create lifting forces [3].

The aircraft's maneuverability will increase when there is an increase in vortex core velocity from the vortex pair on the wing's leading edge. When the roll-up vortex occurs, the axial velocity of the vortex core will be faster than its freestream. In this area, the pressure becomes very low and there arises the an additional lifting force. At specific velocity values and angle of attack, the vortex cores will undergo structural changes and become destroyed due to sudden changes in pressure, the so-called vortex breakdown. In that state, the lift force value will disappear. The flow interaction along the delta wing will affect the formation and character of the vortex core flow. The conditions of axial velocity and the pressure distribution at the vortex core can be used to analyze the vortex core structure and its breakdown. There have been many studies that have been conducted to examine the characteristics of roll-up vortex phenomenon and the occurrence of vortex breakdown to show the aerodynamic character of the delta wing type [4, 5]. Vortex breakdown is used for several analyzes, such as the instability of pressure as well as for the detection of velocity changes [6–8].

Authors of [9] predict the occurrence of a vortex breakdown by analyzing the deceleration of axial velocity changes approaching the freestream. The indication of the occurrence of vortex breakdown is the decrease in axial velocity along the vortex core [9–13]. Detecting the occurrence of vortex breakdown becomes a very important problem that indicates the loss of lifting force on the wing. The flow visualization method is an effective way of determining the vortex breakdown phenomenon. Many methods and researches have been developed to view and analyze the visualization of the occurrence of vortex breakdown, such as the use of wind tunnels, water tunnels or computational fluid dynamics (CFD) methods [14–21]. In [22] the characteristics of the vortex and the effects of some parameters on the form of vortex breakdown have been comprehensively discussed. One of the parameters of the formation of vortex breakdown is the influence of tangential speed and axial velocity along the core of the vortex. Also, one uses swirl ratio or Rossby number to analyze the occurrence of vortex breakdown. The Rossby number (Ro) is a non-dimensional number used for comparison of the axial velocity (U_x) of the vortex core to the maximum swirl velocity (U_θ) of the vortex as formulated in Eq. (1) [22–25]. The decline in the value of Rossby number has the meaning of increased vortex intensity and it further affects the vortex vulnerability. A value criterion of Rossby number showing the occurrence of a vortex breakdown have been proposed in [26] and [27]. The criterion of Rossby number applies to most cases of a vortex in the delta wing with a value

limit of 0.9 and 1.4. The value higher than 1.4 indicates the level of stability of the vortex and the value below 0.9 indicates the occurrence of a vortex breakdown.

$$\mathrm{Ro} = \frac{U_{x(axial)}}{U_{\theta}} . \tag{1}$$

The use of water tunnel is very convenient for studying flow visualization because water has a higher density and lower mass diffusion than air, so that the visualization can be more detailed [19, 28]. However, according to [20], the most difficult part of the measurement on the water tunnel is the pressure measurement, because the operational flow commonly used in water tunnels in of very low order. Besides, due to slower flow, the water tunnel required more meticulous force measuring devices in smaller measuring areas [19]. Test parameters refer to another visualization research using water tunnel with Reynolds number between 10^3–10^4. This value is different and lower than other types of measurements on wind tunnel or real scale, which have higher Reynolds number, and several other studies have shown the suitability of water tunnel test data with real-scale and flight test [14, 19, 29–31].

The use of computational fluid dynamics method (CFD) will be beneficial in presenting the data both qualitatively and quantitatively in a better detail. Wibowo et al. investigated the analysis of the occurrence of vortex breakdown in the delta wing with a sweep angle of 65° and 70° using a water tunnel experimental method and comparing it with CFD testing. He also compared it with references from other studies [17]. The results of the study show a good similarity between the visualization results using water tunnel, CFD, and other references. At a small angle of attack, the results resamble very well the visualization results and lifting forces occurring both on the water tunnel and the CFD method. However, at a high angle of attack after the maximum value of Cl, a slight shift in the lift coefficient value appeaars, which is related to the formation vortex breakdown, thus requiring further research on the computational methods used in particular for the turbulence equations.

Authors of [21] used a CFD technique in modeling to detect the occurrence of a vortex breakdown over the delta wing at a high AoA and to combine it with the addition of jet-flap to see the effect of delay in the occurrence of vortex breakdown. In their study, the model refers to Shih and Ding experiments on wind tunnel testing. The domain model is made in semi-symmetrical form and uses a structured computational mesh type with variations in the number of cells between five hundred and four million cells, with an optimal amount of the mesh of 1.75 million cells. The turbulence model uses low-Reynolds-number stress-omega and low-Reynolds-number eddy-viscosity models. The results show that the use of turbulence model k-ε don't give a proper value for predicting the occurrence of vortex breakdown. Meanwhile, the use of the k-ω model can provide as good results for the calculation and prediction of the beginning of the vortex breakdown

as the results obtained in the experiment. Meanwhile, other researchers also conducted a study to model the development and control of the vortex breakdown phenomenon on the delta wing [3]. The pair of vortices formed on the suction side of the delta wing are significant contributors to the addition of the lift. When the AoA increases, this vorticity becomes stronger and has a high vector value, so that lift force will also increase. The computational model is made using half-symmetry with a mesh number of about 4 million cells. The Navier-Stokes (NS) 3D equation is used to derive the simulation model with the turbulence model using a double eddy-viscosity turbulence (k-ω). A study to see the effectiveness of the use of Spalart-Allmaras (S-A), k-ω, and SST turbulence models on the delta wing have been conducted in [32]. This study compares the lift coefficient and drags coefficient value with that of the wind tunnel model. The results show that, in general, it has not shown a good accuracy, except for a low angle where the use of k-ω and S-A gives good value, while the use of SST model yields an inaccurate value. In other cases, authors of [33] use the S-A turbulence equation to see the aerodynamic characteristics such as the force generated, pressure distribution and streamline visualization of the super-fast car model by arranging the local grid more tightly.

Author of [34] conducted a study using the CFD method, and this study used structured and unstructured mesh types. The turbulence model compares several similarities of both laminar, S-A, k-ε, RSM and LES, and its results are sufficiently accurate, but still not optimal to predict the size and strength of the breakdown vortex. Similarly, the use of the LES model is also not optimal due to the size of the cells that are too large because of a considerable computational load. Simulation of the LES model by refining the local mesh size on the delta 70° wing was presented in [35]. From the results of the study it followed that the use of a rough mesh on the LES model would not produce a good prediction of the vortex, so one should improve the quality of the mesh. Meanwhile, other researchers modeled the turbulence to predict the location of the vortex breakdown using the DES/DDES turbulence model [36]. The results show that the use of DES/DDES predicts the location of the vortex breakdown more accurately and can provide a more reliable flow pattern of the vortices structure and surface pressure distribution.

The phenomenon of fluctuations in velocity and pressure indicates turbulence flow. The modeling for turbulence takes into account several things that include: time-consuming, computational cost, flexibility level, improved physical model accuracy [37]. The case of vortex breakdown in the delta wing shows the dynamic conditions in a stream requiring special treatment in the CFD simulation. The use of appropriate methods will produce optimal results in achieving the results. In this study, we will evaluate the use of some turbulence models available in CFD software to detect the occurrence of vortex breakdown. The results of the study could be a recommendation in the selection of turbulence models of cases of vortex core phenomena and vortex breakdown by considering the accuracy of the results and the computational load.

2. Numerical method

The research process using the numerical method (CFD) starts from the design of the delta wing CAD model with the sweep angle 70°, as shown in Fig. 1a. The half-sectioned model symmetrically refers to the experimental water tunnel data [17]. The completed CAD models and then defines the computational domain with boundary conditions such as inlet, outlet, wall (delta wing) and the walls of symmetry. The mesh is generated on the model by identifying aircraft parts in several blocks based on wing surface changes. The mesh configuration is determined by doing a study on mesh independence. In this case, the required number of cells is at least 5 million cells to achieve the convergence of lift coefficient (Cl) data, as shown in Fig. 1b, and the addition of more cells does not increase the accuracy significantly. Also, testing of the smallest cell dimensions near the wall is also done based on previous studies [38]. Non-dimensional wall distance (y^+) will determine the size of the smallest cell. This determination affects the computational ability in generating a vortex core in the model. Based on previous studies, the smallest optimal size of cells near the wall has a value of $y^+ \leqslant 4$ where the shape of the vortex is still similar to the smallest cell size at $y^+ < 1$. In this study, we use the value $y^+ = 4$ with the smallest cell size of 0.000295 mm.

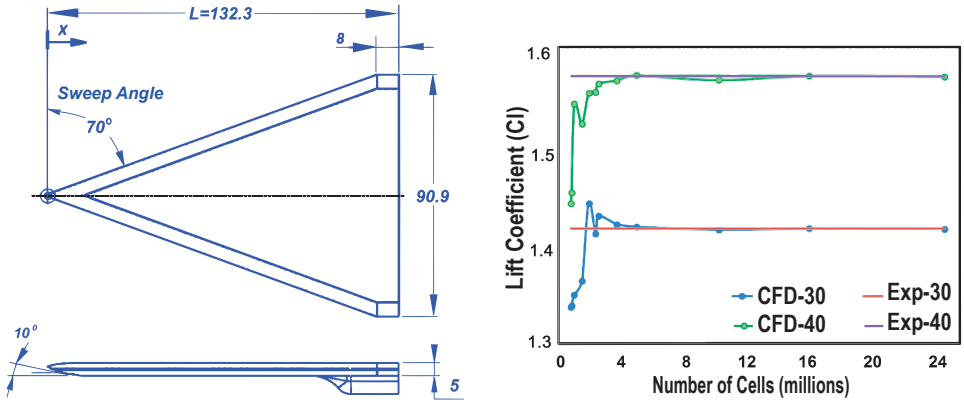

(a) the geometry of the model

(b) mesh independence study for Cl convergence

Fig. 1. Geometry model and mesh independence study of a delta wing with 70° sweep angle

Determination of optimal cell number is done by performing independency mesh study. In this study, it was conducted to find the convergence value of the lift coefficient due to the addition of a cell number. The results showed that the used delta wing model began to converge to a minimum cell number of 5 million cells, as shown in Fig. 2a. In this case, the number of cells used amounted to 6.423 million cells. The mesh type is in the form of a structured-hexahedral mesh

and the cells size changes starting from the wall portion as the smallest size, and evolving logarithmically enlarges to the outside. The domain configuration, shown in Fig. 2b, consists of inlets, outlets, symmetrical sides and walls. Its size is assumed sufficiently large, based on some references, so that inlet, outlet and walls areas do not affect the flow in the model [39–41]. In this research, we used computers with the following specifications: Intel Pentium i7 processor – 3.6 GHz, 32 Gb RAM, 6 TB hard drive by the use of GPU GTX 780 Ti.

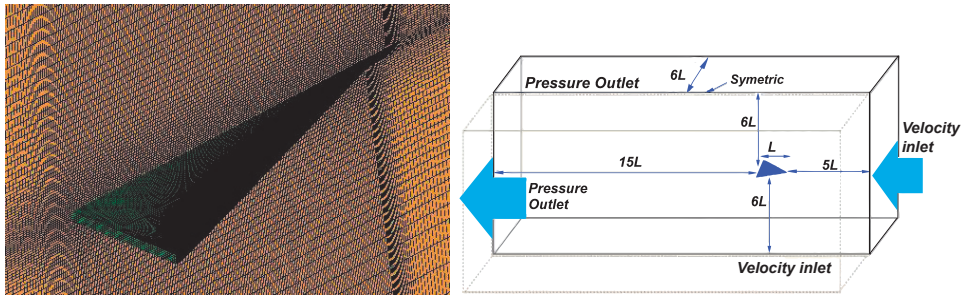

(a) structured-hexahedral mesh (b) CFD boundary condition

Fig. 2. Structured mesh and the domain configuration on the delta wing

In this study, there were several variations of the AoA ranging from 20° to 60° with step 10°. The flow rate was adjusted to inlet velocity of 0.23 m/s (Re = 51582.02) referring to previous study assuming flows on the surface of the wing with 0.08% turbulence intensity [17]. This geometry and condition of this parameter refer to the experimental model. To solve the equation, the numerical solution used the coupled scheme for the settlement of pressure-velocity coupling, with the discretization method using 2nd order upwind. The coupled scheme algorithm solves the momentum equation and the pressure based on continuity pressure equation together. Full implicit coupling was obtained by discretizing the pressure gradient on the momentum equation and with implicit discretization of the face mass flux with turbulence completion using the S-A, k-ε, k-ω, SST, RSM, DDES/SA, and LES equations. This solver scheme offers several advantages over a segregated pressure-based method. This method yields the results more quickly and efficiently especially for single-phase fluids and under steady-state flow conditions.

The results of model simulations were compared with the visualization test using GAMA water tunnel facility. The experiments were carried out by testing the delta wing model in a water tunnel at a velocity of 0.23 m/s and Reynolds number 51582.02 on the AoA 20°, 30°, 40°, and 50°. During the test, the ink flowed out through the ink channel on the model to visualize the flow phenomenon and vortex breakdown above the delta wing surface. The forces that occur on the wing are measured using the 3 DOF force sensors in the water tunnel device [42].

3. Result and discussion

The simulation results provided the lift coefficient (Cl) for each turbulence model with use of Spalart-Allmaras (S-A), k-ε, k-ω, Shear Stress Transport (SST), Reynolds Stress Model (RSM), Delayed Detached Eddy Simulation (DDES/SA), and Large Eddy Simulation (LES). These CFD results, compared with experiment result and several other references presented in [29], are shown in Fig. 3. The results show that the value of Cl increases from the AoA 0° to reach the maximum AoA at 40°. The results show that all of the turbulence models have the value of Cl similar as in the experiment and in another reference. Cl values at a low AoA (0°–20°) have a good similarity across all the turbulence models. At low AoA areas, airflow is still laminar all over the wing.

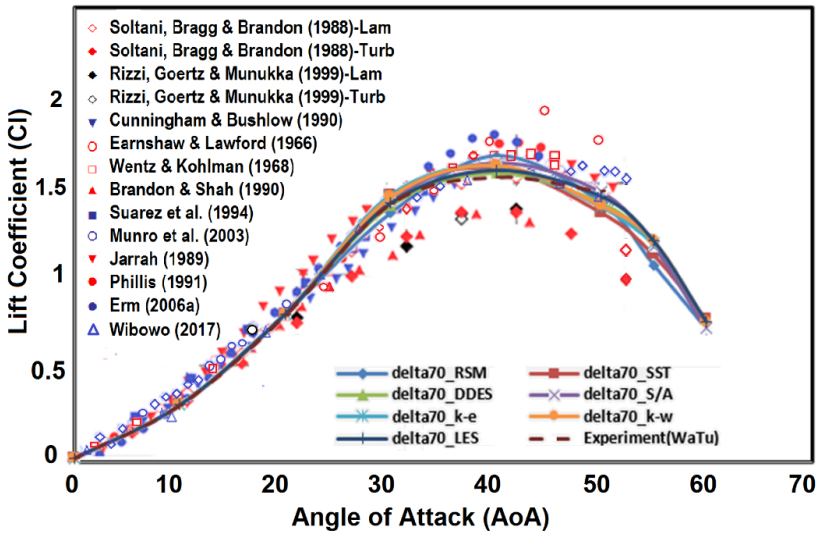

Fig. 3. The value of lift coefficient (Cl) of each form of turbulence model on AoA and compared with other references [29]

The roll-up vortex on the wing at a low AoA is formed continuously and has a vortex core up to the back of the wing, as shown in Fig. 4. In this figure, there are shown the visualization results on a water tunnel and CFD for AoA 20°. The vortex core formed shows a flow like a continuous line and no damage to the vortex core until after passing the delta wing. The visualization shows the laminar flow across the top of the delta wing. In this condition, each turbulence equation has no significant effect on flow conditions. The quantitative result on the coefficient of lift (Cl) also has a very good value for all experiments performed.

At the transition of the AoA that is approaching the maximum lift coefficient (30°–40°), there begins a difference in Cl value in each turbulent model. The difference exists because in most of the flow, especially above the wings and in the

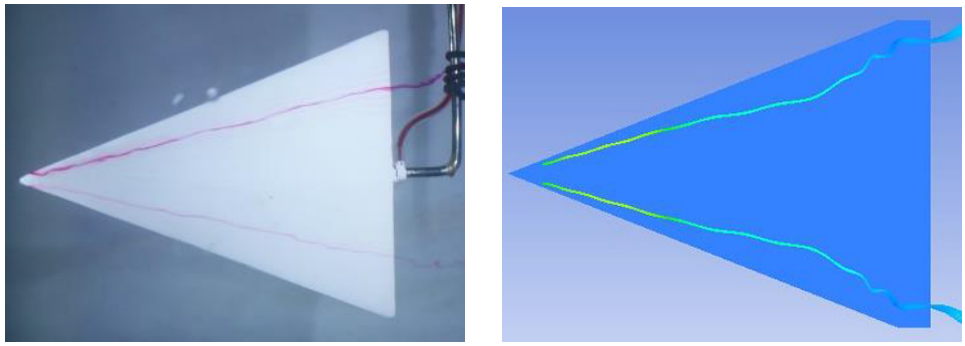

(a) Water tunnel 20° (b) CFD 20° pathline

Fig. 4. The formation of vortex cores at an AoA 20°

back, appears a backflow. The approaches to turbulence model equations solution are different, so they produce different results. This condition is analyzed in detail by looking at the coefficient of lift, by changing the AoA every 2.5 deg in the area, as shown in Fig. 5.

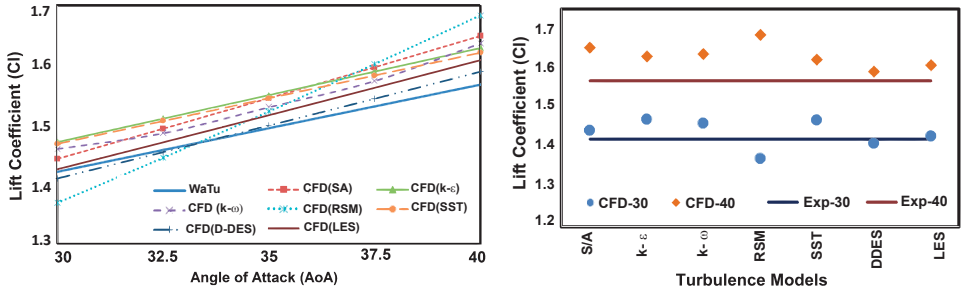

(a) Cl at AoA 30°–40° (b) Cl value comparison

Fig. 5. Details of lift coefficient (Cl) at various turbulent models compared with experiment result (WaTu) (a) from 30°–40°, (b) specific AoA 30° and 40°

In Fig. 5, the coefficient of lift on AoA specific (30°–40°) is compared with the experiment result from the water tunnel (WaTu). The use of the DDES and LES models gives the results very close to the experimental results at both 30° and 40° angles. However, an error increases in the form of LES along with the increase of AoA. Whereas, the turbulent model equation SST, k-ω, and k-ε tend to have a constant value of Cl in the experimental results.

In this study, there are also presented the results of the pressure coefficient (Cp) distribution on the delta wing cross-section, as shown in Fig. 6. The graphs revealed the location of the pressure distribution along the wing cross section in 30% and 60% main wing chords for each turbulence model and the results are compared with the reference [29]. The location of the lowest pressure is the central

location where it produces the largest lift on the wing. From the study, it can be seen that at 30% chord the Cp value can be detected by almost all turbulence equations except on S-A model. Fig. 6a shows that the S-A model is not capable of producing the Cp value corresponding to the experiment. Meanwhile, the magnitude of Cp value can be detected well by DDES model, whereas the equation SST, k-ω, k-ε respectively yields a value lower than the experiment.

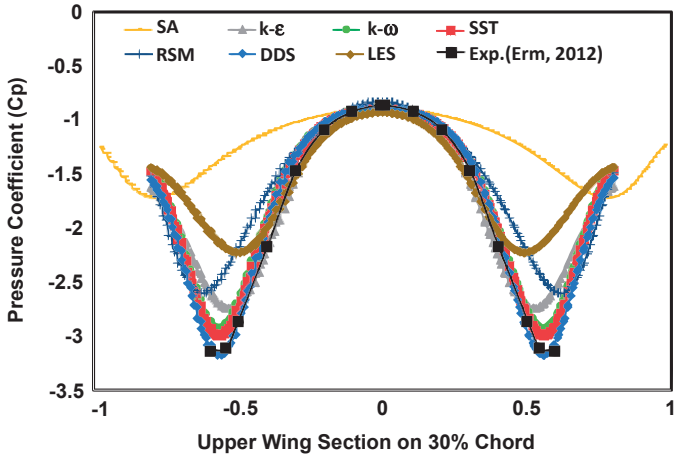

(a)

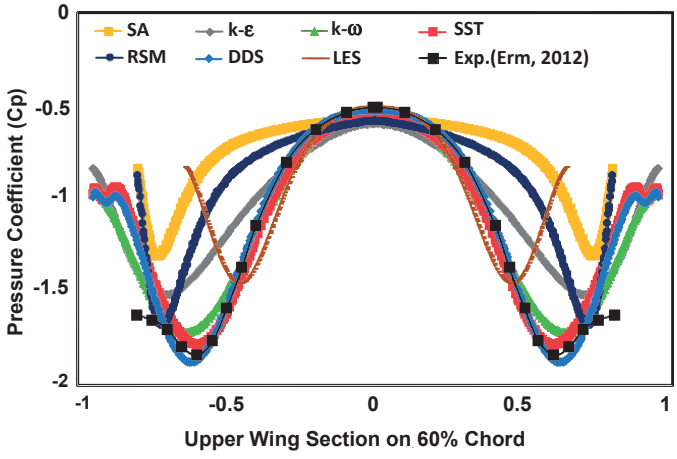

(b)

Fig. 6. Comparison of pressure distribution over the wing section at various turbulence models (CFD) compared with reference [29] on AoA 30° at: (a) 30% mac, (b) 60% chord

At 60% chord (see Fig. 6b), the use of each turbulence equation will produce different Cp values. The use of the DDES model gives results of Cp size and location close to the experimental conditions. The SST, k-ω, and k-ε models provide

a smaller magnitude of Cp value. Whereas, other equations produce the size and location of Cp that is shifted compared to the result of the experiment.

Figs. 7 and 8 show the visualization of the flows over the delta wings at angles of attack 30° and 40° using CFD techniques with various turbulence models and compare the formation of vortex cores with the water tunnel experiment. In the picture presented in CFD method, vortex cores are shown from the path-line movement from the leading edge forming a small vortex to the rear. Whereas, in the water tunnel the formation of the vortex cores is characterized by the ink flow that creates the line.

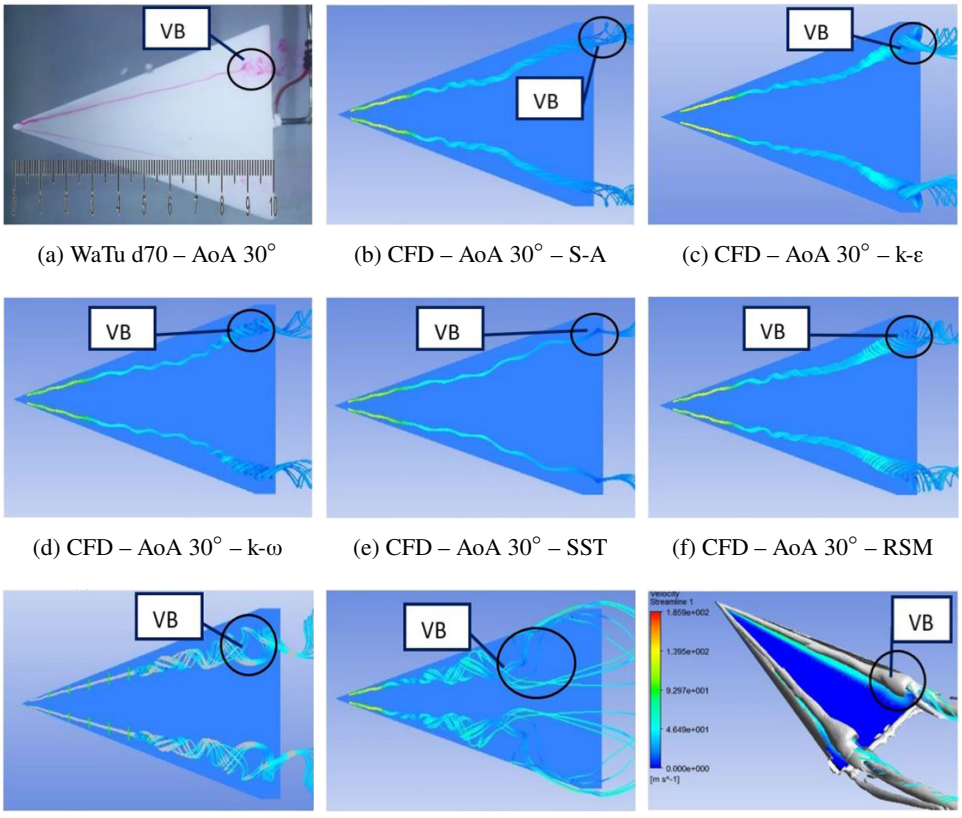

(a) WaTu d70 – AoA 30° (b) CFD – AoA 30° – S-A (c) CFD – AoA 30° – k-ε

(d) CFD – AoA 30° – k-ω (e) CFD – AoA 30° – SST (f) CFD – AoA 30° – RSM

(g) CFD – AoA 30° – DDES/SA (h) CFD – AoA 30° – LES (i) 3D view vortex core

Fig. 7. Comparison of vortex cores and the occurrence of vortex breakdown (VB) in water tunnel experimental (WaTu) and turbulence models (CFD) on AoA 30°

At an AoA of 30°, vortex-core flow visualization begins to exhibit differences in each model, as shown in Fig. 7a. The vortex cores start to appear crushed on the back of the wing. In the water tunnel test, it is clear that there is a fraction of the ink line above the rear wing at the distance to the wing length $(x/L) = 0.87$ indicating the occurrence of vortex breakdown. In the CFD visualization, vortex

breakdown is marked by the presence of a portion of backflow (see Figs. 7b–7h). There are several turbulence models not yet able to predict the occurrence of vortex breakdown as in the S-A equation, while the LES model precedes the destruction of vortex cores. The models of k-ε, k-ω, RSM, SST, D-DES look more closely at the size and location of vortex breakdown, but Fig. 3 shows that there is a difference in Cl that occurs in each equation model. Although the difference is not significant when compared to the values that occur in some references, the results of the DDES model are closest to the phenomenon of the roll-up vortex and the lift force in experimental results. Fig. 7i shows the process of vortex core formation and the occurrence of vortex damage according to Q-criteria analysis.

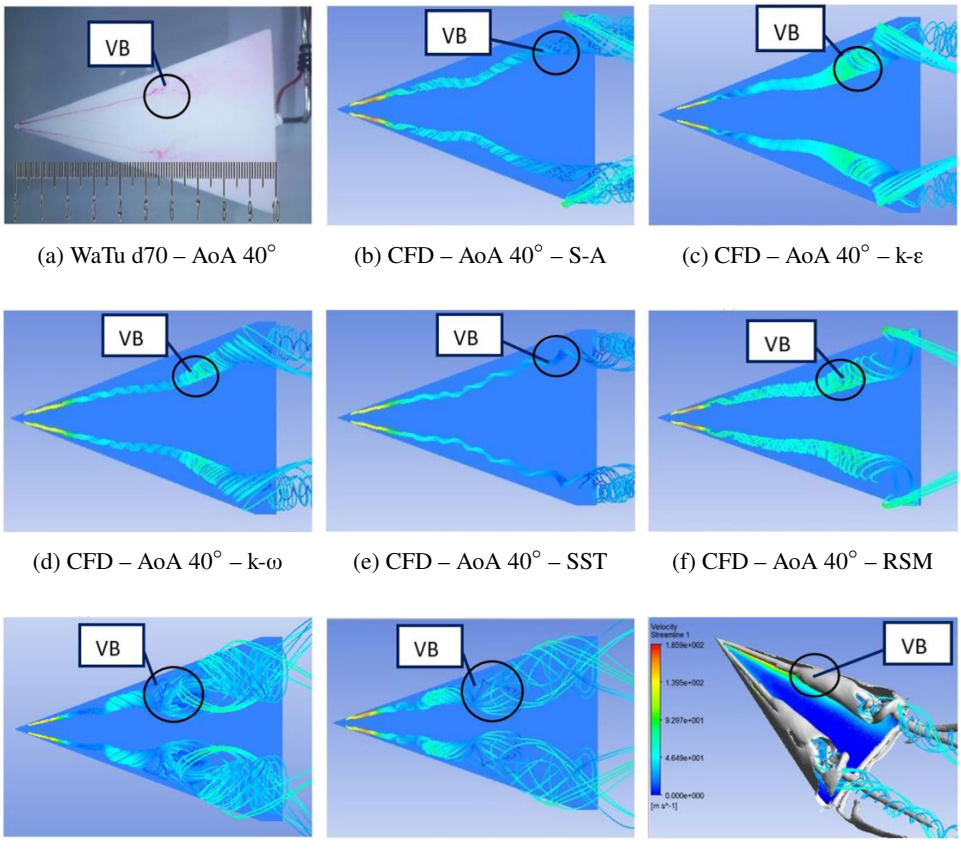

(a) WaTu d70 – AoA 40° (b) CFD – AoA 40° – S-A (c) CFD – AoA 40° – k-ε

(d) CFD – AoA 40° – k-ω (e) CFD – AoA 40° – SST (f) CFD – AoA 40° – RSM

(g) CFD – AoA 40° – DDES/SA (h) CFD – AoA 40° – LES (i) 3D view vortex core

Fig. 8. Comparison of vortex cores and the occurrence of vortex breakdown (VB) in water tunnel experimental (WaTu) and turbulence models (CFD) at AoA 40°

At the AoA of 40° (Fig. 8), it is shown that the vortex core formation in the water tunnel test holds out until x/L is equal to 0.53, then it runs into vortex breakdown. In the CFD test, the S-A turbulence model shows that the formation

of vortex breakdown is delayed compared to the water tunnel experiment. While in other turbulence models vortex breakdown location approaches experimental conditions, DDES and LES provide the best value of the size of vortex breakdown.

Visually, the size and direction of the roll-up of the occurring vortex pathline indicate the formation of vortex breakdown, as shown in Fig. 7 and Fig. 8. Vortex core velocity on the front of the delta wing is higher compared to the velocity of freestream. The phenomenon of the roll-up vortex is causing an increase in vortex core velocity and simultaneously makes the pressure very low above the wing, which creates an increment of the lifting force. Thus, the formation of a roll-up vortex may indicate a higher velocity at the vortex center than the velocity of the free stream.

The increase in Rossby number shows the strength of vortex core velocity against vortex interference that affects vortex core stability. Fig. 9 shows the graph of nondimensional axial velocity value referred to the maximum swirl velocity (U_x/U_θ) depending on Rossby number and vortex breakdown location. Based on a study in [26, 27] about Ro criteria for damage to vortex formation, the figures present the Ro number area for the stability vortex area, instability vortex and vortex breakdown to detect the location of the vortex breakdown. The vortex breakdown value is defined when the Ro < 0.9 indicating that the vortex core velocity has decreased, the vortex instability has increased, and the vortex core has became unformed.

In the areas where we observe a decrease in axial velocity (seen from Ro values less than 0.9), there is the VBL. At AoA 30° (see Fig. 9a), the axial velocity rises starting from the leading edge with the rising Ro number indicating the formation of the vortex core. Next, Ro number decreases to near 0 indicating loss of vortex core and the occurrence of vortex breakdown. For AoA equal to 40° and 50° (see Fig. 9b, 9c) the increase in Ro value is higher, but Ro decreases faster at shorter x/L locations. The location of the vortex breakdown differs between each of the turbulence equations used. Fig. 9d shows a comparison of vortex breakdown (VBL) for a computational model in water tunnel experiments (WaTu) results for AoA 25° to 60°. The comparison of results shows they are similar to the vortex breakdown location at a small AoA. As for high AoA (> 40°), the values of SST, k-ω, and k-ε still show good conformity, while other equations have low accuracy. An excellent match between the DDES turbulence equation model and the experiments exists for each AoA. Similarly, this model shows a good similarity between flow visualization results (Figs. 7 and 8) and pressure distribution (Fig. 6).

In the S-A equation model, the formation of the vortex core is less strong, as seen in the pressure distribution (Fig. 6), and the Ro number distribution (Fig. 9), compared to other equation models. The S-A model results in a slower VBL than in other equations and experiments. The RSM equation model produces vortex core strengths close to that of the DDES model, but the vortex breakdown location is shifted compared to the experiment. The k-ε and k-ω turbulence models have almost identical characteristics that produce less strength of vortex cores, but the

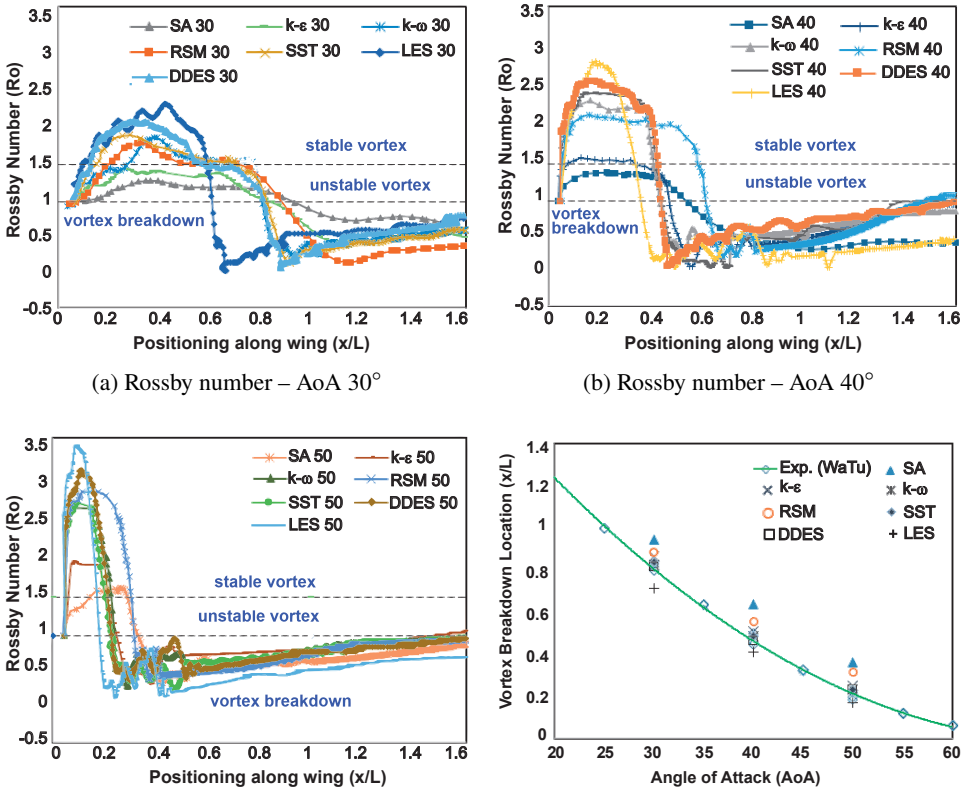

(a) Rossby number – AoA 30°

(b) Rossby number – AoA 40°

(c) Rossby number – AoA 50°

(d) Experiment WaTu and CFD data for VBL

Fig. 9. Distribution of (a, b, c) Rossby number and (d) vortex breakdown location (VBL) the delta wing

location of the vortex breakdown is closer to the experimental conditions. The SST equation is capable of producing a power approaching the DDES equation with the location of the vortex breakdown which is also close to the experimental conditions. Meanwhile, the LES equation produces a stronger vortex core, but vortex breakdown locations occur earlier because LES properties lead to large vortex intensity values.

Table 1 shows the performance time, error rate generated and visualization results of each of the turbulence models used compared to the experiment using water tunnel. In that table, the lift coefficient (Cl) obtained from the CFD simulation at the AoA 30°, 40° and 50° is compared with Cl of the water tunnel experiment, and the difference between the values indicates the error that occurred. The higher the AoA, the higher the error rate that tends to increase due to increased turbulence intensity. The use of the D-DES turbulence equation model ensures the lowest error value of about 1%, while the other model has a higher error value between 4%–7%, but quantitatively the data are still acceptable. As for the results of visualization

analysis based on the location and magnitude of vortex breakdown, one can see that good results occur in the model of SST and DDES. Another factor to consider in computing is the performance time required to complete the computational task. The performance time in Table 1 shows that the S-A, k-ε, and k-ω models have almost the same time requirements, while in the RSM and SST models the times increase slightly, are only twice longer. While, the DDES and LES models require considerable computation times up to 10 times longer compared to those of other models.

Table 1.

The performance time and error values using CFD in each of the turbulence models

Turbulence equation	Error Cl value compare with experiment (water tunnel)				Visualization result	Vortex breakdown location	Performance timer (s)
	30°	40°	50°	Rating			
CFD – SA	2.5%	4.2%	5.7%	Poor	Poor	Poor	379.889
CFD – k/ε	2.5%	3.9%	5.0%	Fair	Good	Good	397.786
CFD – k/ω	2.4%	2.4%	4.0%	Good	Good	Good	460.077
CFD – RSM	5.7%	7.4%	6.6%	Poor	Good	Fair	612.325
CFD – SST	2.3%	2.4%	3.2%	Good	Very good	Good	622.68
CFD – D-DES	0.8%	1.1%	1.2%	Very good	Very good	Very good	7751.234
CFD - LES	0.3%	2.6%	7.6%	Poor	Good	Poor	6429.94

Using the turbulence model to detect the occurrence of vortex breakdown one can see that all turbulence models used are quite acceptable to get quantitative results in calculating the lift coefficient (Cl), especially at a low AoA. However, at a higher AoA, not all the models can predict well the exact occurrence of vortex breakdown. At high AoA, the S-A model there is a lag in results in detecting the occurrence of vortex breakdown. Meanwhile, the LES model, the results are more advanced in the detection of vortex breakdown than the experimental results. The DDES model is the best one both quantitative and qualitative in visualizing the occurrence of vortex cores until vortex breakdown occurs. However, considering very high requirement for computational time, it is necessary to consider the use of other models in predicting the phenomenon of vortex breakdown. The use of SST or k-ω turbulence models is an alternative option for predicting vortex damage with less computational loads.

4. Conclusion

The results show that the use of all turbulence equation in detecting vortex breakdown on delta wing gives quantitatively good results until vortex breakdown. When approaching the vortex breakdown condition, the use of DDES equation gives the best results, both qualitatively and quantitatively, with Cl error value of about 1%. The DDES provides excellent visualization results, but it needs a

considerable computation time. An alternative choice is using the SST or k-ω model, which is a good option for detecting vortex breakdown considering the optimization of computation time required.

Acknowledgments

This work has been carried out with support of the Universitas Gadjah Mada, The Ministry of Research, Technology and Higher Education of the Republic of Indonesia. We would like to express sincere gratitude to Sigit Iswayudi, for time spent in serious discussion, helpful suggestion, and useful conceptual contribution. We sincerely also thank our students C. Wiratama, Zainuri Anwar, Firdaus, and Wega, their help in construction work and conducting data management are gratefully acknowledged.

Manuscript received by Editorial Board, November 06, 2017;
final version, June 06, 2018.

References

[1] E.C. Polhamus. A concept of the vortex lift of sharp-edge delta wings based on a leading-edge-suction analogy. NASA Technical Note D-3767, 1966.

[2] E.C. Polhamus. Vortex lift research: early contributions and some current challenges. In J.F. Campbell, R.F. Osborn, J.T. Foughner Jr., editors, *Vortex Flow Aerodynamics*, NASA Conference Publication 2416, vol. 1, pages 1–30, 1986.

[3] Z. Vlahostergios, D. Missirlis, K. Yakinthos, and A. Goulas. Computational modeling of vortex breakdown control on a delta wing. *International Journal of Heat and Fluid Flow*, 39:64–77, 2013. doi: 10.1016/j.ijheatfluidflow.2012.12.002.

[4] I. Gursul. Review of unsteady vortex flows over delta wings. *21st AIAA Applied Aerodynamics Conference*, pages 1–25, Orlando, USA, 23-26 June 2003. doi: 10.2514/6.2003-3942.

[5] I. Gursul. Review of unsteady vortex flows over slender delta wings. *Journal of Aircraft*, 42(2):299–319, 2005. doi: 10.2514/1.5269.

[6] I. Gursul and H. Yang. Vortex breakdown over a pitching delta wing. *Journal of Fluids and Structures*, 9(5):571–583, 1995. doi: 10.1006/jfls.1995.1032.

[7] M. Menke and I. Gursul. Nonlinear response of vortex breakdown over a pitching delta wing. *Journal of Aircraft*, 36(3):496–500, 1999. doi: 10.2514/2.2481.

[8] P.V Vorobieff and D.O. Rockwell. Vortex breakdown on pitching delta wing: control by intermittent trailing-edge blowing. *AIAA Journal*, 36(4):585–589, 1998. doi: 10.2514/2.409.

[9] M. Chen, P. Liu, H. Guo, and Q. Qu. Effect of sideslip on high-angle-of-attack vortex flow over close-coupled canard configuration. *Journal of Aircraft*, 53(1):217–230, 2016. doi: 10.2514/1.C033305.

[10] V. Mudkavi. The phenomenon of vortex breakdown. In *Proceedings of the Fluid Dynamics Symposium*, pages 123–135, Sikkim, India, 9 July 1993.

[11] E. Krause. A contribution to the problem of vortex breakdown. *Computers & Fluids*, 13(3):375–381, 1985. doi: 10.1016/0045-7930(85)90008-8.

[12] E.A. Anderson and T.A. Lawton. Correlation between vortex strength and axial velocity in a trailing vortex. *Journal of Aircraft*, 40(4):699–704, 2003. doi: 10.2514/2.3148.

[13] T.B. Benjamin. Significance of the vortex breakdown phenomenon. *Journal of Basic Engineering*, 87(2):518–522, 1965. doi: 10.1115/1.3650590.

[14] G.E. Erickson. Water-tunnel studies of leading-edge vortices. *Journal of Aircraft*, 19(6):442–448, 1982. doi: 10.2514/3.57414.

[15] E.D. Robertson, V. Chitta, D.K. Walters, and S. Bhushan. On the vortex breakdown phenomenon in high angle of attack flows over delta wing geometries. In *ASME International Mechanical Engineering Congress and Exposition, Proceedings (IMECE)*, Montreal, Canada, 14–20 November 2014. doi: 10.1115/IMECE2014-39354.

[16] A.M. Thu, Y.H. Byun, and J.-W. Lee. Dye visualization of the vortical flow structure over a double-delta wing. *Journal of Aerospace Engineering*, 25(4):541–546, 2012. doi: 10.1061/(ASCE)AS.1943-5525.0000195.

[17] S.B. Wibowo, Sutrisno, T.A. Rohmat, Z. Anwar, F.R. Syadii, R. Mahardika, and W.F. Naufal. An investigation into the use of GAMA water tunnel for visualization of vortex breakdown on the delta wing. *9th International Conference on Thermofluids, AIP Conference Proceedings*, 2001(1):050007, 2018. doi: 10.1063/1.5049998.

[18] M.H. Sohn, K.Y. Lee, and J.W. Chang. Vortex flow visualization of a yawed delta wing with leading edge extension. *Journal of Aircraft*, 41(2):231–237, 2004. doi: 10.2514/1.9281.

[19] L.P. Erm. Recent aerodynamics research in the dsto water tunnel. In *Proceedings of 16th Australasian Fluid Mechanics Conference*, pages 381–384, Gold Coast, Australia, 2–7 December, 2007.

[20] L.P. Erm. *An investigation into the feasibility of measuring flow-induced pressures on the surface of a model in the AMRL water tunnel*, Report DSTO-TN-0323, 2000.

[21] M. Kyriakou, D. Missirlis, and K. Yakinthos. Numerical modeling of the vortex breakdown phenomenon on a delta wing with trailing-edge jet-flap. *International Journal of Heat and Fluid Flow*, 31(6):1087–1095, 2010. doi: 10.1016/j.ijheatfluidflow.2010.08.002.

[22] J.M. Delery. Aspects of vortex breakdown. *Progress in Aerospace Sciences*, 30(1):1–59, 1994. doi: 10.1016/0376-0421(94)90002-7.

[23] L.A. Schiavetta, O.J. Boelens, S. Crippa, R.M. Cummings, W. Fritz, and K.J. Badcock. Shock effects on delta wing vortex breakdown. *Journal of Aircraft*, 46(3):903–914, 2009. doi: 10.2514/1.38792.

[24] A.M. Mitchell and J. Délery. Research into vortex breakdown control. *Progress in Aerospace Sciences*, 37(4):385–418, 2001. doi: 10.1016/S0376-0421(01)00010-0.

[25] O. Descalzi, J. Martínez, and S. Rica. *Instabilities and Nonequilibrium Structures IX*, Springer, Netherlands, 2012.

[26] R.E. Spall, T.B. Gatski, and C.E. Grosch. A criterion for vortex breakdown. *Physics of Fluids*, 30(11):3434, 1987. doi: 10.1063/1.866475.

[27] B.A. Robinson, R.M. Barnett, and S. Agrawal. Simple numerical criterion for vortex breakdown. *AIAA Journal*, 32(1):116–122, 1994. doi: 10.2514/3.11958.

[28] L.E. Ericsson and J.P. Reding. Unsteady aerodynamics of slender delta wings at large angles of attack. *Journal of Aircraft*, 12(9):721–729, 1975. doi: 10.2514/3.59863.

[29] L.P. Erm and M.V. Ol. An assessment of the usefulness of water tunnels for aerodynamic investigations. Technical Report DSTO-TR-2803, 2012.

[30] J.H. Del Frate, F.A. Zuniga, and D.F. Fisher. In-flight flow visualization with pressure measurements at low speeds on the NASA F-18 high alpha research vehicle. In *AGARD Vortex Flow Aerodynamics Conference*, Scheveningen, Netherlands, 1–4 October, 1990.

[31] O.V. Cavazos Jr. A flow visualization study of LEX generated vortices on a scale model of a F/A-18 fighter aircraft at high angles of attack. Master Thesis, Naval Postgraduate School, Monterey, CA, 1990.

[32] D. Monk and E.A. Chadwick. Comparison of turbulence models effectiveness for a delta wing at low Reynolds numbers. In *7th European Conference for Aeronautics and Space Sciences (EUCASS)*, Milan, Italy, 3–6 July, 2017. doi: 10.13009/EUCASS2017-653.

[33] T. Janson and J. Piechna. Numerical analysis of aerodynamic characteristics of a of high-speed car with movable bodywork elements. *Archive of Mechanical Engineering*, 62(4):451–476, 2015. doi: 10.1515/meceng-2015-0026.

[34] J.A. Freeman. Computational fluid dynamics investigation of vortex breakdown for a delta wing at high angle of attack. Master's Thesis, Air Force Institute of Technology, Ohio, 2003.

[35] I. Mary. Large eddy simulation of vortex breakdown behind a delta wing. *International Journal of Heat and Fluid Flow*, 24(4):596–605, 2003. doi: 10.1016/S0142-727X(03)00053-5.

[36] M. Lv, S. Fang, and Y. Zhang. Numerical simulation of unsteady separated flow over a delta wing using Cartesian grids and DES/DDES. *Procedia Engineering*, 99:423–427, 2015. doi: 10.1016/j.proeng.2014.12.556.

[37] H.K. Versteeg and W. Malalasekera. *An Introduction to Computational Fluid Dynamics – The Finite Volume Method*, 2nd edition Pearson Education, 2007.

[38] Sutrisno, Deendarlianto, T.A. Rochmat, Indarto, S.B. Wibowo, S. Iswahyudi, C. Wiratama and D.B.M. Erlambang. The rolled-up and tip vortices studies in the CFD model of the 3-D swept-backward wind turbine blades. *Modern Applied Science*, 11(12):118–134, 2017. doi: 10.5539/mas.v11n12p118.

[39] J. Franke. Introduction to the prediction of wind loads on buildings by computational wind engineering (CWE). In: Stathopoulos T., Baniotopoulos C.C. (eds), *Wind Effects on Buildings and Design of Wind-Sensitive Structures*, Part of the CISM International Centre for Mechanical Sciences, 493:67–103, 2007. doi: 10.1007/978-3-211-73076-8_3.

[40] J. Revuz, D.M. Hargreaves, and J.S. Owen. On the domain size for the steady-state CFD modelling of a tall building. *Wind and Structures*, 15(4):313–329, 2012. doi: 10.12989/was.2012.15.4.313.

[41] R. Patel and S. Ramani. Determination of optimum domain size for 3D numerical simulation in ANSYS CFX. *International Journal of Innovative Research in Science, Engineering and Technology*, 4(6):1333–1341, 2007.

[42] R.D. Firmansyah, S.B. Wibowo, and R. Mareta. The application of measurement instrument of three degrees of freedom of aerodynamic force in water tunnel. *Jurnal Sains dan Teknologi*, 6(2) Universitas Pendidikan Ganesha, 2017 (in Indonesian). doi: 10.23887/jst-undiksha.v6i2.11785.